Rate Coefficients for the Reactions of Some C_3 to C_5 Hydrocarbon Peroxy Radicals with NO

Jürg Eberhard[†] and Carleton J. Howard*

Aeronomy Laboratory, Environmental Research Laboratories, National Oceanic and Atmospheric Administration, Boulder, Colorado 80303

Received: December 9, 1996; In Final Form: February 19, 1997[⊗]

The rate coefficients for the gas-phase reactions of allyl-, *tert*-butyl-, cyclopentyl-, and 2-pentylperoxy radicals with NO have been measured at 297 ± 2 K in a flow tube reactor using chemical ionization mass spectrometric (CIMS) detection of the peroxy radical. The hydrocarbon radicals were produced through the dissociation of the parent alkyl iodide in a low-power radio frequency (rf) discharge. The unimolecular decomposition of the *c*-pentyl radicals in the rf discharge yielded allyl radicals. The peroxy radicals were generated by reacting the hydrocarbon radicals with O_2. The rate coefficients were found to be, in units of 10^{-12} cm^3 molecule^{-1} s^{-1}, 10.5 ± 1.8, 7.9 ± 1.3, 10.9 ± 1.9, and 8.0 ± 1.4 for the reactions of NO with CH_2═$CHCH_2O_2$, *t*-$C_4H_9O_2$, *c*-$C_5H_9O_2$, and 2-$C_5H_{11}O_2$ radicals, respectively. The results of this study together with our previous results for nonsubstituted C_1-C_3 alkyl peroxy radicals suggest no significant trend in the rate coefficients with size and branching of the radicals. This is in contradiction to some previous studies, which found that the rate coefficients decrease with increasing radical size and complexity. Some implications of this finding for atmospheric chemistry are briefly discussed.

Introduction

Peroxy radicals are intermediates formed in the atmospheric oxidation of hydrocarbons. For example in the case of alkanes, alkyl peroxy radicals are formed through the OH radical initiated oxidation.[1] OH radicals abstract a hydrogen atom from the alkane to form an alkyl radical and water:

$$RH + OH \rightarrow R + H_2O \quad (1)$$

The alkyl radical reacts with O_2 to form an alkyl peroxy radical:

$$R + O_2 \xrightarrow{M} RO_2 \quad (2)$$

In polluted air RO_2 radicals will react predominantly with NO:

$$RO_2 + NO \rightarrow RO + NO_2 \quad (3a)$$

$$\xrightarrow{M} RONO_2 \quad (3b)$$

Reaction 3a is an important step in the formation of photochemical smog since the subsequent photolysis of NO_2 leads to formation of ozone. Reaction 3b acts as a sink for both the alkyl peroxy radical and NO. The rate coefficient ratio k_{3b}/k_{3a} increases monotonically with the carbon number of the peroxy radical, and for example for the 2-pentylperoxy radical it is reported to be ∼0.14 at tropospheric conditions.[2] The ratio k_{3b}/k_{3a} is pressure- and temperature-dependent and is expected to be <0.005 under the experimental conditions employed in this study.[2] At lower concentrations of NO, the reactions of RO_2 radicals with HO_2 radicals, with themselves, and with other organic peroxy radicals represent alternative reaction pathways for RO_2 radicals:

$$RO_2 + HO_2 \rightarrow ROOH + O_2 \quad (4)$$

$$RO_2 + RO_2 \rightarrow \text{products} \quad (5)$$

$$RO_2 + R'O_2 \rightarrow \text{products} \quad (6)$$

Especially with regard to less polluted air, it is important to know the relative rates of reactions 3 through 6.

The overall rate coefficients k_3 for the *t*-$C_4H_9O_2$ + NO and the *i*-$C_3H_7O_2$ + NO reactions have been measured at 290 K by Peeters et al.[3] Their value for the latter rate coefficient is about a factor 2 lower than our previous measurements obtained using chemical ionization mass spectrometry (CIMS).[4,5] From the measurements of Peeters et al. and from measurements of the rate coefficients of the $(CH_3)_3CCH_2O_2$ + NO and $(CH_3)_3CC(CH_3)_2CH_2O_2$ + NO reactions by Sehested et al.[6], it has been suggested that the rate coefficients for RO_2 + NO reactions decrease with increasing size and branching of the alkyl group.

Also of interest is the reaction of allylperoxy radicals, $C_3H_5O_2$, with NO. The atmospheric oxidation of isoprene, CH_2═$C(CH_3)CH$═CH_2, through OH radicals leads to the formation of complex peroxy radicals that contain hydroxy and/or C═C functionalities in the β-position to the peroxy group.[1,7,8] Isoprene is one of the most abundant non-methane hydrocarbons of biogenic origin in the atmosphere. While the reactions of representative OH-substituted RO_2 radicals with themselves and with HO_2 radicals have been studied,[8] no reactions of NO with RO_2 radicals containing the C═C functionality have yet been examined. These complex radicals are difficult to isolate in the laboratory, and therefore the $C_3H_5O_2$ radical was chosen as a surrogate to investigate the effect of the β-C═C functionality on the reactivity of the peroxy radical.[9,10] The reactions of the $C_3H_5O_2$ radical with itself[9,10] and with HO_2 radicals[10] have been investigated. By comparing the reactivity of the $C_3H_5O_2$ radical to that of its saturated analogue, the *n*-$C_3H_7O_2$ radical, Boyd et al.[10] found an increase in the self-reaction rate coefficient of about a factor of 3. The room-temperature reaction rate

[†] Fellow of the Schweizerischer Nationalfonds zur Förderung der wissenschaftlichen Forschung. Present address: Department of Chemistry, National Tsing Hua University, Hsinchu, Taiwan 30043, Republic of China.

* To whom correspondence should be addressed at: NOAA, ERL, 325 Broadway R/E/AL2, Boulder, CO 80303. Fax: (303)497-5822. E-mail: howard@al.noaa.gov.

[⊗] Abstract published in *Advance ACS Abstracts,* April 1, 1997.

S1089-5639(96)04028-5 CCC: $14.00

coefficients of organic peroxy radical reactions with HO_2 radicals appear to be insensitive to the degree of substitution of the organic group.[8] The only trend observed is an increase in the rate coefficients with increasing size of the radical up to a limiting value for radicals containing four or more carbon atoms. The results for the $C_3H_5O_2 + HO_2$ reaction are in accord with those findings.[10]

In the present study our objective is to determine rate coefficients for the reactions of some larger nonsubstituted RO_2 radicals with NO in order to investigate possible structure−reactivity relationships. To study the effect of increasing size of the radical along with branching and cyclic vs straight-chain configurations, we choose *t*-$C_4H_9O_2$, *c*-$C_5H_9O_2$, and 2-$C_5H_{11}O_2$ radicals as model species on the basis of the availability of iodide precursors and as being representative of radicals present in the atmosphere. Previously, we reported studies of the reactions of NO with CH_3O_2,[11] $C_2H_5O_2$,[5] *n*-$C_3H_7O_2$,[5] *i*-$C_3H_7O_2$,[4,5] and $CH_3C(O)O_2$[12] radicals.

Experimental Section

Apparatus. The experimental system has been used previously to study the kinetics of $RO_2 + NO$ reactions.[4,5,11,12] The apparatus consists of a neutral flow tube reactor coupled to an ion flow tube/quadrupole mass spectrometer commonly referred to as a flowing afterglow.[13] Both the flowing afterglow technique[13] and flow tube kinetic measurements using CIMS[14] have been described previously. Recent papers describe most details of the flowing afterglow[15] and the neutral flow tube[11] used in this study.

Detection Scheme. The peroxy radicals, RO_2, were detected as their parent anion RO_2^- according to the reaction:

$$RO_2 + O_2^- \rightarrow RO_2^- + O_2 \qquad (7)$$

The signal at the corresponding mass was attributed to the radical by procedures described before.[4] The generation of O_2^- reagent ions is accomplished by attaching electrons to O_2 as described previously.[4,5] Under some experimental conditions involving the largest [NO] an unidentified background at the RO_2^- mass was observed (up to 14% of the initial radical signal in the case of *t*-$C_4H_9O_2$ radicals, up to 2% in the case of 2-$C_5H_{11}O_2$ radicals, and up to 8% in the case of $C_3H_5O_2$ and *c*-$C_5H_9O_2$ radicals). The background signal arises from the rf discharge source, as it was not observed from the reaction of the precursor iodide with O_2^-. Some of the measurements involving the largest [NO] and radical decays were corrected for the background signal as described in the Results section.

Radical Generation. The peroxy radicals were generated by reacting the hydrocarbon radicals with O_2, as shown in reaction 2. Initially, attempts were made to generate C_5 alkyl radicals from the pyrolysis of C_6 alkyl nitrites, e.g.,

$$CH_3(CH_2)_2CH(CH_2ONO)CH_3 \xrightarrow{\Delta} CH_3(CH_2)_2CHCH_3 + H_2CO + NO \qquad (8)$$

as employed previously in this laboratory to generate C_1 to C_3 alkyl radicals.[4,5,11] We were unable to detect any signal at a mass corresponding to a C_5 alkylperoxy radical. This is most probably due to the unimolecular decomposition of the alkyl radicals at the elevated temperatures in the pyrolysis source, e.g.,

$$CH_3(CH_2)_2CHCH_3 \xrightarrow{\Delta} C_2H_5 + C_3H_6 \qquad (9)$$

Dearden and Beauchamp[16] studied reaction 9 at 623 and 773 K using photoelectron spectroscopy. At the higher temperature, comparable to our conditions, the 2-pentyl radical signal almost disappeared, whereas the ethyl radical and propylene signals increased compared to the levels they observed at the lower temperature.

TABLE 1: Experimental Conditions for Radical Generation

organic precursor	He flow through reservoir (STP cm^3 s^{-1})	He flow added after reservoir (STP cm^3 s^{-1})
tert-butyl iodide	0	3.5−4.5
iodocyclopentane	0.1−0.2	7.0−9.0
2-iodopentane	0.1−0.2	6.5−7.5

In the present study, hydrocarbon radicals were generated in a low-power (∼5 W) radio frequency discharge through dissociation of the parent alkyl iodide as we described recently for the generation of C_2H_5 and *i*-C_3H_7 radicals.[5] Some unimolecular decomposition of the hydrocarbon radicals also occurs in this radical source, as we observed signals corresponding to smaller RO_2 radicals in addition to the signals for the RO_2 parent radicals intended for study. For example, upon generation of *tert*-butyl radicals, we also observed a signal at *m*/*e* 47 corresponding to $CH_3O_2^-$. Methyl radicals are likely to be formed through the following reaction:[17]

$$(CH_3)_3C \xrightarrow{\Delta} CH_3 + CH_3CH{=}CH_2 \qquad (10)$$

Upon generation of *c*-pentyl radicals we also observed signals at *m*/*e* 73 corresponding to $C_3H_5O_2^-$ and *m*/*e* 47 corresponding to $CH_3O_2^-$. Allyl radicals are formed through the following reaction:[18]

$$c\text{-}C_5H_9 \xrightarrow{\Delta} CH_2CH{=}CH_2 + C_2H_4 \qquad (11)$$

The source of methyl radicals from *c*-C_5H_9 radicals is unknown. Upon generation of 2-pentyl radicals, we also observed signals corresponding to $CH_3O_2^-$, $C_2H_5O_2^-$, and $C_3H_7O_2^-$. The corresponding alkyl radicals are formed from the decomposition of the 2-pentyl radical, either directly or following an internal 5−2 hydrogen transfer.[16]

Experimental Conditions. Helium flow rates of 12−34 STP cm^3 s^{-1} (STP ≡ 273 K, 1 atm) and pressures of 1.9−4.1 Torr were used in the neutral flow tube. These conditions resulted in flow speeds of 1100−2470 cm s^{-1}. NO flow rates ranging from 2×10^{-4} to 5×10^{-3} STP cm^3 s^{-1} were introduced to the flow tube through the movable injector, yielding [NO] = 6×10^{11} to 2×10^{13} molecules cm^{-3} in the neutral tube. The NO was delivered from a cylinder,[4] through a dry ice cooled silica gel filled trap.

The organic precursors were eluted from reservoirs kept at 273 K at conditions summarized in Table 1. An additional He flow was added after the reservoir and before the discharge source to decrease the residence time in the radical source and to reduce the loss of radicals to self-reaction and loss to the wall of the tube. Rate coefficients for the hydrocarbon radical self-reactions are known for the C_3H_5 radical, $k_{298K} = 3.0 \times 10^{-11}$ cm^3 $molecule^{-1}$ s^{-1},[9] and for the *t*-C_4H_9 radical, $k_{308K} = 8.2 \times 10^{-12}$ cm^3 $molecule^{-1}$ s^{-1}.[19] The concentration of the alkyl iodide precursor is not known accurately. If we assume that the vapor pressures of the precursor compounds are comparable to those of 1-iodo-2-methylpropane and 1-iodo-3-methylbutane, for which they are known,[20] we estimate rf discharge dissociation efficiencies ranging from about 10% to 50%. O_2 was added to the source reactor at a flow rate of 1 STP cm^3 s^{-1}, resulting in O_2 concentrations in the radical source of 7×10^{15} to 2×10^{16} molecules cm^{-3}. Under these conditions

>99.9% of the hydrocarbon radicals are converted to RO_2 radicals before they enter the reaction zone of the neutral flow tube, assuming a rate coefficient $>8 \times 10^{-13}$ cm^3 molecule^{-1} s^{-1} for the reaction of the radical with O_2. This is the case for the reaction of O_2 with *t*-C_4H_9[21] and *c*-C_5H_9[22] radicals and is assumed to be true also in the case of 2-C_5H_{11} radicals. In the case of C_3H_5 radicals 95% of the radicals are converted to peroxy radicals before the reaction zone under worst case assumptions. For this estimate the smaller rate coefficient for the O_2 addition to C_3H_5 radicals from Ruiz et al.,[23] measured at 2.8 Torr and 348 K, is preferred over the value determined by Jenkin et al.[9] at atmospheric pressure and 296 K. From the value by Ruiz et al.[23] we estimate $k_{298K} = 2.5 \times 10^{-13}$ cm^3 molecule^{-1} s^{-1}. The total initial concentrations of RO_2 radicals in the reactor, $[RO_2]_{tot}$, were estimated to be in the range 9×10^{10} to 4×10^{11} molecules cm^{-3} assuming one NO_2 molecule produced per RO_2 radical reacted via reaction 3 and measuring the product $[NO_2]$ as described previously.[4]

Materials. The following radical source materials were used without further purification: *tert*-butyl iodide (Aldrich, ≥95%), 2-iodopentane (Pfaltz and Bauer, ≥97%), and iodocyclopentane (Pfaltz and Bauer, ≥92%). The other gases were as described previously.[4]

Results

The RO_2 radicals were generated in the radical source at a fixed position on the flow tube. NO was added through the movable injector. [NO] was in excess over $[RO_2]_{tot}$ by a factor of 5−120 so that the reaction kinetics were pseudo-first-order in the total peroxy radical concentration. The variation of the concentration of an individual radical with reaction time is described by eqs I and II,[11]

$$d[RO_2]dt = -k[RO_2] \quad \text{(I)}$$

$$\ln[RO_2] = -kt + c \quad \text{(II)}$$

where $k = k_3[NO] - k_w$, c is a constant, k_3 is the bimolecular rate coefficient for reaction 3, and k_w is the first-order rate coefficient for loss of peroxy radicals on the wall of the movable injector. The wall loss on the injector enters because the amount of injector surface exposed to the radical stream decreases as the injector is moved to increase the reaction time. The first-order rate coefficient k_w is determined by measuring the RO_2 radical decay when [NO] = 0 and is found to be small with values < 3 s^{-1}. The reaction time is varied by changing the NO injector position in the reaction zone of the flow tube. A series of decay plots are taken at different NO concentrations. A series of typical decay plots are shown in Figure 1, where the log of the $C_3H_5O_2^-$ signal (*m*/*e* 73) is plotted vs the relative reaction time on a linear scale. Note that the decrease in the *m*/*e* 73 signal with increasing [NO] at zero relative reaction time in Figure 1 is due to further reaction between the last injector position defined here as $t = 0$ and the true zero time position, where the gas from the radical reactor enters the ion flow tube. Thus the decay plots in Figure 1 all extrapolate to a common point corresponding to the true zero on the time coordinate. The measurements involving larger [NO] shown in Figure 1 are influenced by the background signal and therefore show curved decays. A nonweighted nonlinear least squares fit of a particular decay determines k for the corresponding NO concentration. The fitting of the decays involving larger [NO] showing curvature was carried out using an additional fitting parameter for the background signal. This procedure was applied to typically the two largest decays of one series of

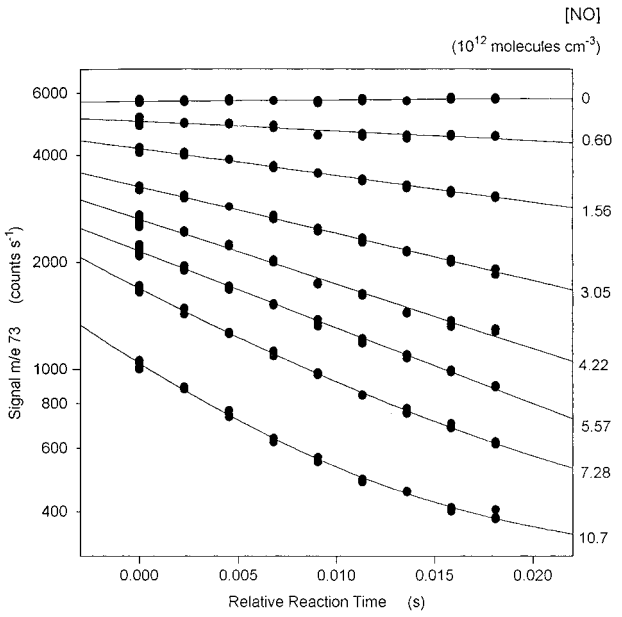

Figure 1. Typical semilog plots of the $C_3H_5O_2^-$ (*m*/*e* 73) signal vs relative reaction time. Conditions were $v = 2210$ cm s^{-1}, $p = 2.02$ Torr, and [NO] = (0−10.7) × 10^{12} molecules cm^{-3} as indicated to the right of each decay. The lines are nonlinear least squares fits.

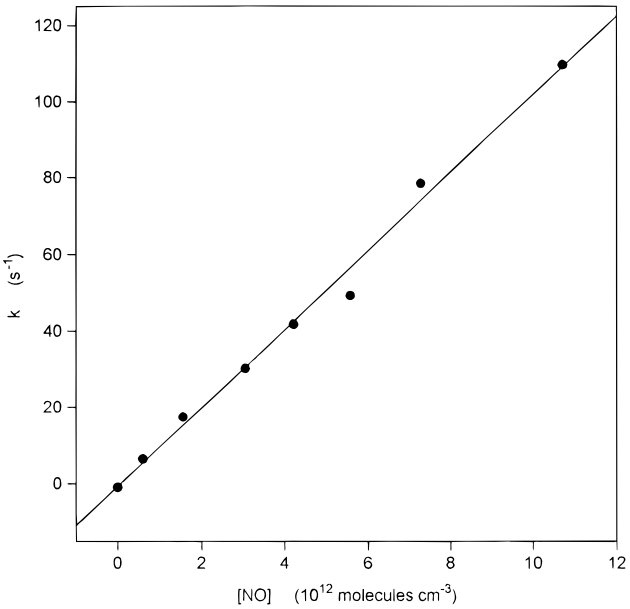

Figure 2. Typical plot of k vs [NO] for the $C_3H_5O_2$ + NO reaction. The k values are from nonlinear least squares fits of the decays shown in Figure 1. A linear least squares fit of the data shown gives a bimolecular rate coefficient k_3 of (10.3 ± 0.7) × 10^{-12} cm^3 molecule^{-1} s^{-1}, where the error limits represent 2 standard errors.

decays. The background was determined individually in all these cases and was found to vary from one series of decays to another, probably indicating that this signal arises from the radical source as the conditions for the radical generation were varied from one series to another. In Figure 2, the k values from Figure 1 are plotted against their NO concentrations. Note that the two values at the highest [NO], for which the background correction was applied, fall on the line determined by the values at lower [NO]. The slope of the linear least squares fit to this plot is the bimolecular rate coefficient k_3 for the reaction of $C_3H_5O_2$ radicals and NO. The k axis intercept of this fit determines k_w. Table 2 summarizes all the experiments carried out at 297 ± 2 K. The averages for the rate coefficients are (in units of 10^{-12} cm^3 molecule^{-1} s^{-1}) 10.5 ±

TABLE 2: Summary of Experiments; All Results Were Determined at 297 ± 2 K

RO_2 radical	number of expts	p (torr)	flow speed (cm s^{-1})	[NO] range (10^{12} molecules cm^{-3})	k_3[a] (10^{-12} cm^3 $molecule^{-1}$ s^{-1})
t-$C_4H_9O_2$	8	1.94	1970	1.0−10.5	8.10 ± 0.72
	7	2.10	1580	2.2−12.8	7.80 ± 1.22
	7	1.96	1960	1.9−15.0	8.45 ± 0.56
	8	2.51	2470	1.9−9.7	7.65 ± 1.26
	8	2.99	1100	1.5−9.4	7.67 ± 0.50
				average	7.9 ± 1.3[c]
2-$C_5H_{11}O_2$	7	2.13	2210	1.2−7.2	7.52 ± 0.80
	7	2.08	1530	1.4−7.3	8.29 ± 1.10
	7	2.60	2200	1.6−8.3	8.30 ± 0.84
	8	3.09	1670	1.2−5.8	7.98 ± 0.52
	7	4.07	1810	1.6−9.5	7.90 ± 0.30
				average	8.0 ± 1.4[c]
c-$C_5H_9O_2$	7	2.02	2210	0.6−10.7	10.9 ± 0.4
	8	1.98	1430	0.9−6.6	11.3 ± 0.7
	8	2.65	2130	1.8−8.4	10.7 ± 0.7
	7	3.05	1660	1.1−9.7	10.3 ± 0.8
	7	3.97	1670	1.3−8.4	11.2 ± 0.7
				average	10.9 ± 1.9[c]
CH_2═CH-CH_2O_2[b]					10.3 ± 0.7
					10.2 ± 1.0
					10.2 ± 1.3
					11.1 ± 0.9
					10.5 ± 0.6
				average	10.5 ± 1.8[c]

[a] Error limits are 2 standard errors from linear least-squares fits of *k* vs [NO] plots. [b] Experimental conditions were the same as for *c*-$C_5H_9O_2$. [c] Recommended value: average of all measurements with error bars of ±17%, as described in text.

0.8, 7.9 ± 0.7, 10.9 ± 0.8, and 8.0 ± 0.6 for the reactions of NO with CH_2═$CHCH_2O_2$, *t*-$C_4H_9O_2$, *c*-$C_5H_9O_2$, and 2-$C_5H_{11}O_2$ radicals, respectively. The error bars given here represent 2 standard deviations. We estimate the overall uncertainty in k_3 to be ±17% at the 95% confidence level.[11] Using these error bars, we recommend the following rate coefficients in units of 10^{-12} cm^3 $molecule^{-1}$ s^{-1} for the reactions of NO with CH_2═$CHCH_2O_2$, *t*-$C_4H_9O_2$, *c*-$C_5H_9O_2$, and 2-$C_5H_{11}O_2$ radicals, respectively: 10.5 ± 1.8, 7.9 ± 1.3, 10.9 ± 1.9, and 8.0 ± 1.4.

Discussion

An rf discharge source was used to prepare the hydrocarbon radicals in this study. Although pyrolysis of alkyl nitrites was used successfully in our previous studies of the CH_3O_2,[11] $C_2H_5O_2$,[5] *n*-$C_3H_7O_2$,[5] and *i*-$C_3H_7O_2$[4] radical reactions with NO, we found that the alkyl radicals C_4H_9 and larger were subject to extensive fragmentation in the pyrolysis source. This is probably the result of the unimolecular rates for fragmentation being larger than or comparable to the rates for decomposition of the parent nitrite compounds in the furnace. Some fragmentation of the alkyl radicals was observed in the rf discharge source, but satisfactory levels of reactant radicals could be prepared from the iodide compounds.

The rf power is maintained at a low level and the extent of fragmentation in the rf source is less than observed in the pyrolysis source. The rate coefficient for the CH_3O_2 + NO reaction was measured in this study for CH_3 fragments from all three precursors and found to be about 8 × 10^{-12} cm^3 $molecule^{-1}$ s^{-1}, which is in good agreement with our preferred measurement of (7.5 ± 1.3) × 10^{-12} cm^3 $molecule^{-1}$ s^{-1} obtained using a different radical source and precursor and ion detection scheme.[11] In this case the results are probably unaffected by secondary chemistry, because the initial CH_3O_2 concentration from the source seems to be higher than the concentration of the larger parent RO_2 radicals. The signal for $CH_3O_2^-$ was typically a factor of 5−10 times larger than the signal of the parent RO_2 radical intended for study. The individual radical concentrations were not determined, but the total RO_2 concentration, $[RO_2]_{tot}$, was evaluated by converting RO_2 to NO_2 via reaction 3 and measuring the NO_2 yield by CIMS. The unimolecular decomposition of product alkoxy radicals, RO, formed through reaction 3a can lead to the formation of smaller alkyl radicals, R′,[1] which can form other RO_2 radicals via reaction with excess O_2 present in the flow reactor. However it is unlikely that either the ion detection scheme or the radical source is affected by secondary chemistry in this study.

The fragmentation of *c*-C_5H_9 was used as a source for the allyl radical C_3H_5. An important requirement for this source to be successful in kinetics measurements is that the fragmentation of the parent *c*-$C_5H_9O_2$ reaction product does not lead to the formation of C_3H_5 in the reactor. The product of the *c*-$C_5H_9O_2$ + NO reaction is the cyclopentylalkoxy radical, *c*-C_5H_9O, which can react by opening the ring and forming CH_2-$CH_2CH_2CH_2CHO$ or via reaction with O_2, forming HO_2 radicals and cyclopentanone. Neither of these compounds is likely to decompose forming C_3H_5, and we observed no evidence of such a reaction. Rowley et al.[24] studied the kinetics and products of the cyclopentylperoxy radical self-reaction. Using FTIR spectroscopy at 700 Torr, they found that the cyclopentoxy radical product undergoes ring opening. They did not report observing products that indicate significant fragmentation of the C_5 chain.

Table 3 summarizes all the room-temperature data for RO_2 + NO reactions for nonsubstituted hydrocarbon radicals obtained in this laboratory using CIMS along with literature data. Note that all the data reported by Adachi and Basco[37−39] have been excluded from Table 3, as their measurements seem to be affected by a systematic error.[40] A graphic representation of data from Table 3 is given in Figure 3. The CH_3O_2 + NO reaction has been the subject of several investigations. With the exception of the high value obtained by Masaki et al.,[33] all rate coefficient values are in agreement within the experimental uncertainties, with an average value of 7.8 × 10^{-12} cm^3 $molecule^{-1}$ s^{-1}. Masaki et al. used pulsed laser photolysis combined with photoionization mass spectrometry. The reason for the disagreement between the value determined by Masaki et al. and the average value is not known. There are five determinations of the $C_2H_5O_2$ + NO reaction rate coefficient with all the values being in fairly good agreement. The average value is 9.0 × 10^{-12} cm^3 $molecule^{-1}$ s^{-1}.

Our room-temperature rate coefficient of (7.9 ± 1.3) × 10^{-12} cm^3 $molecule^{-1}$ s^{-1} for the *t*-$C_4H_9O_2$ + NO reaction is about a factor of 2 higher than the value of (4.0 ± 1.1) × 10^{-12} cm^3 $molecule^{-1}$ s^{-1} measured by Peeters et al.[3] A difference of the same order is found in our rate coefficient values for the *i*-$C_3H_7O_2$ + NO reaction.[4,5] Peeters et al.[3] determined the rate coefficients from the NO_2 product growth profile using a flow reactor with molecular beam sampling mass spectrometry. They generated alkyl radicals through reaction of the appropriate alkene with H atoms formed in a microwave discharge. The radicals formed in this manner are highly excited, but are believed to be relaxed by collisions with the bath gas and not to be significantly fragmented. They corrected the NO_2^+ signal for influences from secondary reactions and for contributions of NO_2^+ fragment ions from organic nitrates and peroxynitrates. Unaccounted for reactions of NO_2 could lead to errors in their analysis, although the magnitude of the corrections they apply appears to be small compared to the factor of 2 discrepancy with our result. In the present study the peroxy radical signal was measured directly and was corrected for a background only

TABLE 3: Summary of Room-Temperature Rate Coefficient Data for RO_2 + NO Reactions for Nonsubstituted Radicals; Data by Adachi and Basco[37−39] Excluded

R	$k_{298} \times 10^{12}$ (cm^3 molecule^{-1} s^{-1})	method[a]	monitored species	ref
CH_3	8.0 ± 2.0	DF-EIMS	RO_2	25
	7.1 ± 1.4	FP-UV	RO_2	26
	6.5 ± 2.0	MMS	RO_2	27
	7.7 ± 0.9	FP-UV	RO_2	28
	8.6 ± 2.0	DF-EIMS	RO_2	29
	8.1 ± 1.6	LP-LIF	NO_2	30
	7 ± 2	LP-LA	RO_2	31
	8.8 ± 2.2[b]	PR-UV	NO_2	6
	9.1 ± 2.0	DF-EIMS	RO_2	32
	11.2 ± 1.4	LP-PIMS	RO_2	33
	7.5 ± 1.3	FT-CIMS	RO_2	11
C_2H_5	8.9 ± 3.0	DF-EIMS	NO_2	34
	8.5 ± 2.1[b]	PR-UV	NO_2	6
	8.2 ± 1.6	DF-LIF	RO	35
	10.0 ± 1.9[c]	LP-IR/UV	NO/RO_2	36
	9.3 ± 1.6	DF/FT-CIMS	RO_2	5
CH_2=$CHCH_2$	10.5 ± 1.8	DF-CIMS	RO_2	this work
n-C_3H_7	9.4 ± 1.6	FT-CIMS	RO_2	5
i-C_3H_7	5.0 ± 1.2	DF-EIMS	NO_2	3
	9.0 ± 1.6	FT-CIMS	RO_2	4
	9.1 ± 1.5	DF-CIMS	RO_2	5
t-C_4H_9	4.0 ± 1.1	DF-EIMS	NO_2	3
	7.9 ± 1.3	DF-CIMS	RO_2	this work
c-C_5H_9	10.9 ± 1.9	DF-CIMS	RO_2	this work
2-C_5H_{11}	8.0 ± 1.4	DF-CIMS	RO_2	this work
$(CH_3)_3CCH_2$	4.7 ± 1.2[b]	PR-UV	NO_2	6
$(CH_3)_3CC(CH_3)_2CH_2$	1.8 ± 0.5[b]	PR-UV	NO_2	6

[a] DF = discharge flow, FP = flash photolysis, LP = laser photolysis, PR = pulse radiolysis, FT = flow tube, EIMS = electron impact mass spectrometry, UV = ultraviolet absorption, MMS = molecular modulation spectroscopy, LIF = laser-induced fluorescence, LA = laser absorption, PIMS = photoionization mass spectrometry, CIMS = chemical ionization mass spectrometry, IR = infrared absorption. [b] Error bars represent overall uncertainty of ±25% as estimated by Sehested et al.[6] [c] Derived from the room-temperature measurements of Maricq and Szente[36] with overall error of ±19%. The room-temperature rate coefficient derived from their Arrhenius expression is 9.4×10^{-12} cm^3 molecule^{-1} s^{-1}.

at low signal levels. Another major difference in the experimental setup is that Peeters et al. add O_2 and NO together to the flow tube to form RO_2 radicals from the alkyl radicals. In view of the rather high RO_2 concentration of 3×10^{12} molecules cm^{-3} employed, their kinetics could be affected by radical−radical and secondary reactions. Because their result is based upon the measurement of the NO_2 product and radical reactants are not observed, we believe the discrepancy may be due to reactions of unknown species in their experiments. It should be noted, however, that Peeters et al.[3] also reported the rate coefficient for the CF_3O_2 + NO reaction using detection of both the CF_3O_2 reactant radical and the NO_2 product and obtained a result in excellent agreement with several other laboratories including ours.[41]

Sehested et al.[6] reported rate coefficients for a number of RO_2 + NO reactions. Among the radicals they studied are the hydrocarbon peroxy radicals CH_3O_2, $C_2H_5O_2$, $(CH_3)_3CCH_2O_2$, and $(CH_3)_3CC(CH_3)_2CH_2O_2$. Sehested et al. used pulsed radiolysis radical generation with time-resolved near UV spectroscopy to measure the NO_2 product formation rates. Their analysis included modeling and making corrections for secondary and competing reactions. As shown in Table 3 and Figure 3, their results for the smaller peroxy radicals, CH_3O_2 and $C_2H_5O_2$, agree well with the other studies, but the C_5 and C_8 peroxy radicals show markedly decreased reactivity. They concluded that their data indicated a trend with the rate constants

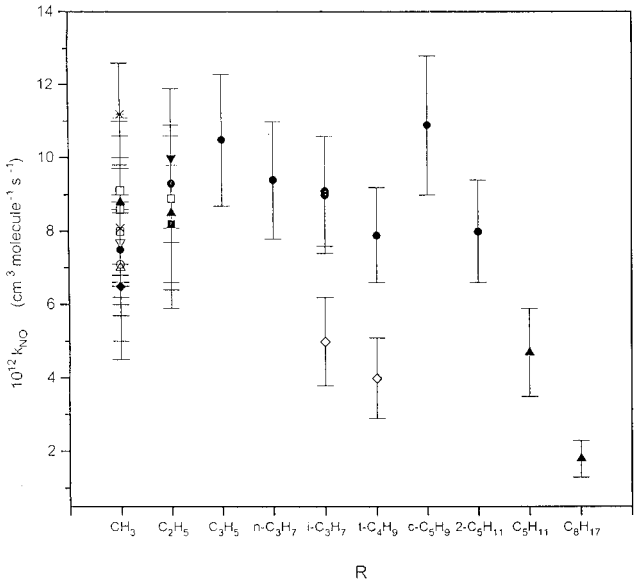

Figure 3. Graphic representation of all room-temperature rate coefficient data on RO_2 + NO reactions for nonsubstituted hydrocarbon radicals given in Table 3: (●) this laboratory,[4,5,11,this work] (□) CSIRO group,[25,29,32,34] (○) Sander and Watson,[26] (◆) Cox and Tyndall,[27] (▽) Simonaitis and Heicklen,[28] (×) Ravishankara et al.,[30] (△) Zellner et al.,[31] (▲) Sehested et al.,[6] (*) Masaki et al.,[33] (■) Daële et al.,[35] (▼) Maricq and Szente,[36] and (◇) Peeters et al.[3]

decreasing with increasing alkyl chain length and branching. Unfortunately, neither of the large radicals, $C_5H_{11}O_2$ or $C_8H_{17}O_2$, studied by Sehested et al.[6] were available for the present measurements, so a direct comparison cannot be made. Because none of the larger radicals studied here are the same as those studied by Sehested et al., it is possible there is no discrepancy between their work and ours.

We know of no previous studies of the rate coefficients for the reactions of NO with CH_2=$CHCH_2O_2$, *c*-$C_5H_9O_2$, and 2-$C_5H_{11}O_2$ radicals. As shown in Figure 3, the rate coefficients for the CH_2=$CHCH_2O_2$ + NO and *c*-$C_5H_9O_2$ + NO reactions are slightly higher than the other measurements carried out in this laboratory. The RO_2 + NO rate coefficient data obtained in this laboratory for saturated hydrocarbon radicals do not show a trend with increasing size and branching of the radical. This is in contradiction to the earlier findings of Peeters et al.[3] and Sehested et al.,[6] who found that the rate coefficients decrease with increasing size and branching of the molecule and attributed this trend to a steric effect. In both studies the rate of formation of the NO_2 product was followed, and obtaining the rate coefficients for reaction 3 required modeling of the raw data. Assuming there is a discrepancy in the trends observed in those studies compared to the present work, it could imply the following: (i) the generation of the larger radicals leads to interferences not significant or possibly not present in the small radical systems; (ii) the modeling of the results is based on an inaccurate reaction scheme and/or erroneous rate coefficients.

Some evidence that the reported decrease in the RO_2 + NO rate coefficient with the size and complexity of the R is not a steric effect is found in a recent series of studies of RO_2 + NO and RO_2 + NO_2 reactions, where the R group is derived from an ether. The studies were made using the pulse-radiolysis radical generation and near UV absorption detection of NO_2 as employed by Sehested et al.[6] Three different ether molecules were studied: (a) dimethyl ether (DME) CH_3OCH_3,[42] (b) methyl *tert*-butyl ether (MTBE) $CH_3OC(CH_3)_3$,[43] and (c) di-*tert*-butyl ether (DTBE), $(CH_3)_3COC(CH_3)_3$.[44] In these studies both the RO_2 + NO and RO_2 + NO_2 rate coefficients were reported. The RO_2 + NO_2 reaction is an association reaction and exhibits

TABLE 4: Comparison of Indirect Measurements of the Rate Coefficients for the Reactions of RO_2 with NO and NO_2 at 296 K and 1 atm of SF_6

radical (RO_2)	$k(RO_2 + NO)$ (10^{-12} cm^3 molecule^{-1} s^{-1})	$k(RO_2 + NO_2)$ (10^{-12} cm^3 molecule^{-1} s^{-1})	ref
CH_3OCH_2OO	9.1 ± 1	7.9 ± 0.4	42
$CH_3OC(CH_3)_2CH_2OO$	4.3 ± 1.6	12 ± 3	43
$(CH_3)_3COC(CH_3)_2CH_2OO$	1.8 ± 0.2	9.9 ± 1.3	44

a pressure dependence at low pressures, but since these studies were carried out in one atmosphere of SF_6, a highly efficient bath gas, the reactions are expected to be at or near the high-pressure limit, k_∞. The crux of our argument is that the $RO_2 + NO$ and $RO_2 + NO_2$ reactions are very similar in that both occur on attractive radical−radical recombination surfaces. In the case of $RO_2 + NO$, the energetic bound complex [ROONO] has sufficient energy above the threshold for dissociation into $RO + NO_2$ products and does so with a high efficiency. In the case of $RO_2 + NO_2$, the energetic complex [RO_2NO_2] does not have an exothermic metathesis channel but can dissociate back to reactants or be stabilized by bath gas collisions. The high pressure limit rate coefficient is the complex formation rate coefficient. To a first approximation, one expects the rate coefficients for these two processes to be quite similar, and they are usually within a factor of 2 or so.[40] The point is that both reactions should exhibit similar steric tendencies.

The results from the pulse-radiolysis studies of the ether-based $RO_2 + NO$ and NO_2 reactions are summarized in Table 4. Although the $RO_2 + NO$ rate coefficient decreases by about a factor of 5 with increasing R size and complexity, the $RO_2 + NO_2$ reaction rate coefficients are the same, 1×10^{-11} cm^3 molecule^{-1}s^{-1} within about 20%. The authors attribute the change in $RO_2 + NO$ reactivity to a steric effect,[43] but this is not reasonable because the $RO_2 + NO_2$ reactions should exhibit a similar tendency, if it were a steric effect. The main difference between the $RO_2 + NO$ and $RO_2 + NO_2$ reaction is in the chemistry: the former is a chain-propagating reaction leading to the formation of more and smaller RO_2 species, while the latter is a simple radical chain-terminating reaction. We have observed a tendency toward increasing fragmentation of the R group with increasing size of R. We believe that the studies by Peeters et al.[3] and Sehested et al.[6] that derive the rate coefficient from the rate of appearance of the NO_2 product are likely to have more interference from fragmentation and secondary chemistry with the large R groups.

We do not believe there is a systematic error in the present results. The reactant peroxy radical species are detected directly, and the reported rate coefficients are determined from their removal rates. We are unable to find a plausible scheme to explain how the reaction rates of the larger radicals could appear to be accelerated as required to explain the discrepancies with the trends in the studies of Peeters et al.[3] and Sehested et al.[6] It should be noted that a direct comparison of rate coefficient measurements leads to a disagreement for only two radicals, the isopropylperoxy and *tert*-butylperoxy radicals both of which were also studied by Peeters et al.[3] Otherwise the reactivity trends are derived from comparing different hydrocarbon groups.

Temperature-dependent data are available for the CH_3O_2,[11] $C_2H_5O_2$,[5,36] *n*-$C_3H_7O_2$,[5] and *i*-$C_3H_7O_2 + NO$[4] reactions, with all showing values of E/R in the range of −(270 to 380) K. Similar small negative temperature dependencies have also been found for the reaction of NO with other peroxy radicals, such as, HO_2,[45,46] $CH_3C(O)O_2$,[12] and CF_3O_2.[40] We expect the E/R values for all the nonsubstituted, saturated aliphatic RO_2 radicals to be generally in this range, −(250 to 400) K.

The major role of the $RO_2 + NO$ reaction in the atmosphere is to oxidize NO to NO_2 and to propagate the photooxidation of the organic fragment. The RO product typically reacts with O_2 to form HO_2 and an aldehyde or ketone or fragments to form a carbonyl compound and an organic radical, which immediately produces a new $R'O_2$ radical.[47] Thus the reaction with NO leads to ozone production via photolysis of the NO_2 product and the continued generation of peroxy radicals and oxidation of the organic fragment. In the remote troposphere, where the mole fraction of NO falls below about 100 ppt (parts per trillion), the $RO_2 + NO$ reaction competes with the reactions of RO_2 with HO_2 and other RO_2 species. In general the HO_2 reaction yields an organic hydroperoxide, ROOH, and the $RO_2 + R'O_2$ reactions yield a mixture of alcohols, carbonyls, and oxide radicals.[48] The relative rates of these competing reactions are extremely important for assessing the rate of ozone production and the photooxidation rates of atmospheric organic compounds. If our finding that the reactivity of RO_2 toward NO is not decreased as the R group becomes larger and more complex is correct, the $RO_2 + NO$ reactions will play a more important role in the remote and clean regions with low concentrations of NO. There will be more ozone production and more rapid photooxidation of the organic radicals.

If one assumes $k_4(RO_2 + HO_2)$ is typically about 10^{-11} cm^3 molecule^{-1} s^{-1},[48] our conclusion that the $RO_2 + NO$ rate coefficient is typically 8×10^{-12} cm^3 molecule^{-1} s^{-1} suggests that even in the remote troposphere with a low [NO], the NO reaction effectively competes with the HO_2 reaction. Cantrell et al.[49] report $RO_2 + HO_2$ mole fractions of about 25 ppt and NO mole fractions of about 10−20 ppt from measurements at a clean Pacific site. Assuming the HO_2 is about one-fifth of the total peroxy radical concentration, the $RO_2 + NO$ rate will exceed the $RO_2 + HO_2$ rate, if k_3 is about 8×10^{-12} cm^3 molecule^{-1} s^{-1}, but will not if k_3 falls below about 4×10^{-12} cm^3 molecule^{-1} s^{-1}. Jenkin and Hayman[8] and Boyd et al.[10] estimated the importance of the different loss processes, reactions 3−6, for the RO_2 radicals formed from the OH radical initiated oxidation of isoprene. They assumed rate coefficients of 4×10^{-12} cm^3 molecule^{-1} s^{-1} for the $RO_2 + NO$ reactions. These RO_2 radicals contain five carbon atoms and either a hydroxy or C=C or both functionalities. From our results, we predict reaction 3 to be a more important loss reaction for these radicals by a factor of about 2−2.6 compared to the estimates by Jenkin and Hayman and Boyd et al. This in turn implies enhanced O_3 formation via photolysis of the NO_2 product arising from the OH radical initiated oxidation of isoprene.

In summary, the results of this study together with our previous measurements for C_1 to C_3 radicals[4,5,11] represent a set of measurements for the reactions of C_1 to C_5 hydrocarbon peroxy radicals with NO. The rate coefficients for the reactions of NO with nonsubstituted saturated aliphatic peroxy radicals are all found to be on the order of 8×10^{-12} cm^3 molecule^{-1} s^{-1}. For modeling of atmospheric processes,we suggest that the rate coefficients for these reactions can be assumed to be the same. The effect of the larger rate coefficients reported here, compared to the previous results,[3,6] which indicated that the larger and more complex R groups reacted more slowly, is to increase the effectiveness of the $RO_2 + NO$ reactions relative to other loss processes for RO_2 radicals. The larger fraction of RO_2 radicals reacting with NO will lead to the formation of more O_3 via photolysis of the NO_2 product and more rapid breakdown of the R group since the RO radicals are known to be highly reactive.[1] Further studies are planned to investigate the effects of other functional groups and radical size upon the $RO_2 + NO$ reactivity.

Acknowledgment. The authors thank Dr. L. G. Huey for technical assistance and Dr. E. R. Lovejoy for helpful discussions. J.E. would like to thank the Schweizerische Nationalfonds zur Förderung der wissenschaftlichen Forschung for a fellowship. This work was supported in part by the NOAA Climate and Global Change Program.

References and Notes

(1) Atkinson, R. *J. Phys. Chem. Ref. Data* **1994**, Monograph No. 2.
(2) Carter, W. P. L.; Atkinson, R. *J. Atmos. Chem.* **1989**, *8*, 165.
(3) Peeters, J.; Vertommen, J.; Langhans, I. *Ber. Bunsen-Ges. Phys. Chem.* **1992**, *96*, 431.
(4) Eberhard, J.; Villalta, P. W.; Howard, C. J. *J. Phys. Chem.* **1996**, *100*, 993.
(5) Eberhard, J.; Howard, C. J. *Int. J. Chem. Kinet.* **1996**, *28*, 731.
(6) Sehested, J.; Nielsen, O. J.; Wallington, T. J. *Chem. Phys. Lett.* **1993**, *213*, 457.
(7) Paulson, S. E.; Seinfeld, J. H. *J. Geophys. Res.* **1992**, *97*, 20703.
(8) Jenkin, M. E.; Hayman, G. D. *J. Chem. Soc., Faraday Trans.* **1995**, *91*, 1911.
(9) Jenkin, M. E.; Murrells, T. P.; Shalliker, S. J.; Hayman, G. D. *J. Chem. Soc., Faraday Trans.* **1993**, *89*, 433.
(10) Boyd, A. A.; Nozière, B.; Lesclaux, R. *J. Chem. Soc., Faraday Trans.* **1996**, *92*, 201.
(11) Villalta, P. W.; Huey, L. G.; Howard, C. J. *J. Phys. Chem.* **1995**, *99*, 12829.
(12) Villalta, P. W.; Howard, C. J. *J. Phys. Chem.* **1996**, *100*, 13624.
(13) Ferguson, E. E.; Fehsenfeld, F. C.; Schmeltekopf, A. L. *Adv. At. Mol. Phys.* **1969**, *5*, 1.
(14) Gleason, J. F.; Sinha, A.; Howard, C. J. *J. Phys. Chem.* **1987**, *91*, 719.
(15) Huey, L. G.; Hanson, D. R.; Howard, C. J. *J. Phys. Chem.* **1995**, *99*, 5001.
(16) Dearden, D. V.; Beauchamp, J. C. *J. Phys. Chem.* **1985**, *89*, 5359.
(17) Birrell, R. N.; Trotman-Dickenson, A. F. *J. Chem. Soc.* **1960**, 4218.
(18) Gordon, A. S. *Can. J. Chem.* **1965**, *43*, 570.
(19) Anastasi, C.; Arthur, N. L. *J. Chem. Soc., Faraday Trans. 1* **1987**, *83*, 277.
(20) *CRC Handbook of Chemistry and Physics*, 72nd ed.; CRC Press Inc.: Boca Raton, 1991.
(21) (a) Lenhardt, T. M.; McDade, C.; Bayes, K. D. *J. Chem. Phys.* **1980**, *72*, 304. (b) Wallington, T. J.; Andino, J. M.; Potts, A. R. *Int. J. Chem. Kinet.* **1992**, *24*, 649.
(22) Wu, D.; Bayes, K. D. *Int. J. Chem. Kinet.* **1986**, *18*, 547.
(23) Ruiz, R. P.; Bayes, K. D.; Macpherson, M. T.; Pilling, M. J. *J. Phys. Chem.* **1981**, *85*, 1622.
(24) Rowley, D. M.; Lightfoot, P. D.; Lesclaux, R.; Wallington, T. J. *J. Chem. Soc., Faraday Trans.* **1992,** *88*, 1369.
(25) Plumb, I. C.; Ryan, K. R.; Steven, J. R.; Mulcahy, M. F. R. *Chem. Phys. Lett.* **1979**, *63*, 255.
(26) Sander, S. P.; Watson, R. T. *J. Phys. Chem.* **1980**, *84*, 1664.
(27) Cox, R. A.; Tyndall, G. S. *J. Chem. Soc., Faraday Trans. 2* **1980**, *76*, 153.
(28) Simonaitis, R.; Heicklen, J. *J. Phys. Chem.* **1981**, *85*, 2946.
(29) Plumb, I. C.; Ryan, K. R.; Steven, J. R.; Mulcahy, M. F. R. *J. Phys. Chem.* **1981**, *85*, 3136.
(30) Ravishankara, A. R.; Eisele, F. L.; Kreuter, N. M.; Wine, P. H. *J. Chem. Phys.* **1981**, *74*, 2267.
(31) Zellner, R.; Fritz, B.; Lorenz, K. *J. Atmos. Chem.* **1986**, *4*, 241.
(32) Kenner, R. D.; Ryan, K. R.; Plumb, I. C. *Geophys. Res. Lett.* **1993**, *20*, 1571.
(33) Masaki, A.; Tsunashima, S.; Washida, N. *Chem. Phys. Lett.* **1994**, *218*, 523.
(34) Plumb, I. C.; Ryan, K. R.; Steven, J. R.; Mulcahy, M. F. R. *Int. J. Chem. Kinet.* **1982**, *14*, 183.
(35) Daële, V.; Ray, A.; Vassalli, I.; Poulet, G.; Le Bras, G. *Int. J. Chem. Kinet.* **1995**, *27*, 1121.
(36) Maricq, M. M.; Szente, J. J. *J. Phys. Chem.* **1996**, *100*, 12374.
(37) Adachi, H.; Basco, N. *Chem. Phys. Lett.* **1979**, *63*, 490.
(38) Adachi, H.; Basco, N. *Chem. Phys. Lett.* **1979**, *64*, 431.
(39) Adachi, H.; Basco, N. *Int. J. Chem. Kinet.* **1982**, *14*, 1243.
(40) Atkinson, R.; Baulch, D. L.; Cox, R. A.; Hampson, R. F.; Kerr, J. A.; Troe, J. *J. Phys. Chem. Ref. Data* **1992**, *21*, 1125.
(41) Bevilacqua, T. J.; Hanson, D. R.; Howard, C. J. *J. Phys. Chem.* **1993**, *97*, 3750.
(42) Langer, S.; Tjungstrom, E.; Ellerman, T.; Nielsen, O. J.; Sehested, J. *Chem. Phys. Lett.* **1995**, *240*, 53.
(43) Langer, S.; Tjungstrom, E.; Ellerman, T.; Nielsen, O. J.; Sehested, J. *Chem. Phys. Lett.* **1995**, *240*, 499.
(44) Nielsen, O. J.; Sehested, J.; Langer, S.; Tjungstrom, E.; Wangberg, I. *Chem. Phys. Lett.* **1995**, *238*, 359.
(45) Howard, C. J. *J. Chem. Phys.* **1979**, *71*, 2352.
(46) Seeley, J. V.; Meads, R. F.; Elrod, M. J.; Molina, M. J. *J. Phys. Chem.* **1996**, *100*, 4026.
(47) Atkinson, R.; Carter, W. P. L. *J. Atmos. Chem.* **1991**, *13*, 195.
(48) Lightfoot, P. D.; Cox, R. A.; Crowley, J. N.; Destriau, M.; Hayman, G. D.; Jenkin, M. E.; Moortgat, G. K.; Zabel, F. *Atmos. Environ.* **1992**, *26A*, 1805.
(49) Cantrell, C. A.; Shetter, R. E.; Gilpin, T. M.; Calvert, J. G. *J. Geophys. Res.* **1996**, *101*, 14643.